Single and low-lying states dominance in two-neutrino double-beta decay

O. Moreno,[1] R. Álvarez-Rodríguez,[2] P. Sarriguren,[1] E. Moya de Guerra,[3] F. Šimkovic,[4] and A. Faessler[5]

[1]*Instituto de Estructura de la Materia, CSIC, Serrano 123, E-28006 Madrid, Spain*
[2]*Department of Physics and Astronomy, University of Aarhus, DK-8000 Aarhus C, Denmark*
[3]*Departamento de Física Atómica, Molecular y Nuclear, Universidad Complutense de Madrid, E-28040 Madrid, Spain*
[4]*Department of Nuclear Physics, Comenius University, SK-842 15 Bratislava, Slovakia*
[5]*Institut für Theoretische Physik, Universität Tübingen, D-72076 Tübingen, Germany*

(Dated: November 3, 2008)

A theoretical analysis of the single-state dominance hypothesis for the two-neutrino double-beta decay rates is performed on the examples of the double-beta decays of ^{100}Mo, ^{116}Cd, and ^{128}Te. We also test the validity of an extended low-lying-state dominance that takes into account the contributions of the low-lying excited states in the intermediate nucleus to the double-beta decay rates. This study has been accomplished for all the double-beta emitters for which we have experimental information on their half-lives. The theoretical framework is a proton-neutron quasiparticle random-phase approximation based on a deformed Skyrme Hartree-Fock mean field with pairing correlations. Our calculations indicate that there are not clear evidences for single- or low-lying-state dominance in the two-neutrino double-beta decay. Finally, we investigate the single electron energy distributions of the outgoing electrons in the double-beta decay processes with an exact treatment of the energy denominators, which could help to a more comprehensive analysis of NEMO-3 data.

PACS numbers: 21.60.Jz;23.40.Hc;27.60.+j

I. INTRODUCTION

The nonzero mass of the neutrino has been recently confirmed by neutrino oscillation experiments [1], where neutrinos created in a flavor eigenstate are subsequently found to be in various flavors. However, these experiments can only probe differences of squared neutrino masses, but not the absolute neutrino mass scale, which remains still unknown. The neutrinoless double-beta ($0\nu\beta\beta$) decay nuclear process [2, 3, 4] is considered to be one of the most suitable candidates to provide this information. $0\nu\beta\beta$ decay is a lepton-number violating mode, which is forbidden in the Standard Model and that only occurs if neutrinos are massive Majorana particles. The half-life of this process involves an effective neutrino mass that could be eventually extracted from the measured half-lives.

Since the double-beta decay process is necessarily dependent on the nuclear structure properties, lack of accuracy in the determination of the nuclear matrix elements involved in the process is a source of uncertainty in the information on neutrino properties that can be extracted from $0\nu\beta\beta$ decay experiments. Contrary to the $0\nu\beta\beta$ decay, the double-beta decay with the emission of two (anti)neutrinos ($2\nu\beta\beta$) can proceed as a perturbative process in the Standard Model and has indeed been observed in several nuclides. This Standard Model allowed form of the decay is used as a test for the nuclear models considered. The operators involved in the 0ν and 2ν modes are different. In the 2ν decay mode the operator connects the initial and final 0^+ states via virtual 1^+ transitions to the intermediate nucleus. In the 0ν decay mode the transitions to the intermediate nucleus may take place to many different multipolarities. Nevertheless, the underlying nuclear structure involved in both processes is similar. Success in describing the 2ν decay mode is a requirement for a reliable calculation of the nuclear matrix elements related to the $0\nu\beta\beta$ decay.

The nuclear structure calculation involved in the $2\nu\beta\beta$ decay is not an easy task. Being a second order process in the weak interaction, the nuclear matrix elements involve a summation over the full set of virtual nuclear 1^+ states in the odd-odd intermediate nucleus. Two leading microscopic nuclear models are commonly used to evaluate the nuclear matrix elements involved in the decay process. They are the nuclear shell model [5, 6] and the proton-neutron quasiparticle random-phase approximation (pnQRPA)[7, 8, 9, 10]. The shell model approach takes into account all possible correlations but within a restricted valence space. It successfully describes the low-lying excited states, but has difficulties with the description of states at high excitation energies, in particular, in the region of the Gamow-Teller (GT) resonance for open-shell medium and heavy nuclei, where most of the double-beta emitters are located. On the other hand, pnQRPA calculations do not have these problems related to the limited model space, but relevant ground state correlations might be missing. In addition, these calculations are very sensitive to model parameters. One problem of the theoretical $2\nu\beta\beta$ decay studies is whether the contributions of higher-lying states to the $2\nu\beta\beta$ decay amplitude, which are apparently disfavored by large energy denominators, play an important role. As we have mentioned, this has important consequences on the reliability of the shell model and pnQRPA to describe the nuclear matrix elements.

In the eighties, Abad and collaborators suggested [11] that in those cases where the ground state of the odd-odd intermediate nucleus is a 1^+ state reachable by a GT transition, the transition through it could account for the major part of the $2\nu\beta\beta$ matrix element. This conjecture is called the single-state dominance (SSD) hypothesis. If SSD hypothesis is confirmed, the half-lives for $2\nu\beta\beta$ decay could be determined from single β^- and electron capture (EC) measurements, experiments which are in principle much easier to carry out than the elaborated and time-consuming double-beta decay experiments. On the theoretical side, the possible realization of the SSD hypothesis for the ground-state to ground-state transitions would lead to a drastic simplification in the theoretical description of the intermediate nucleus, since now only the lowest 1^+ wave function has to be calculated. If SSD is valid, this would increase the reliability of the small valence spaces used in the full shell model calculations.

From the experimental point of view, early tests of the SSD hypothesis were evaluated on the $2\nu\beta\beta$ decay of ^{100}Mo and ^{116}Cd, two cases where the ground state of the intermediate odd-odd nucleus is $J^\pi = 1^+$. In Refs. [12] and [13], the EC half-lives of the ground state of the intermediate nucleus, ^{100}Tc and ^{116}In respectively, were measured. Combining these measurements with the already known β^- half-lives, the SSD hypothesis was confirmed to some extent on those examples. Experimental information on the EC and β^- decay of ^{128}I is also available [14].

Theoretically, the SSD hypothesis was systematically studied in Ref. [15] within a pnQRPA formalism. The analysis performed there showed that the SSD hypothesis is realized in most cases but the mechanism leading to this property is not unique. In some instances the SSD is realized through a true dominance of the first 1^+ virtual state, while in other cases it is realized due to cancellations among the contributions from higher lying 1^+ states of the intermediate nucleus. However, one should notice that the theoretical formalism used in Ref. [15], is complemented with some adjusting of the single-particle levels around the proton and neutron Fermi surfaces to reproduce the observed single-quasiparticle spectrum. In addition, the scaling factor of the strength in the particle-particle residual force is fixed in each nucleus by optimizing the agreement with the experimentally known EC and β^- decay rates. This indicates that the theoretical evidences of the SSD hypothesis claimed in Ref. [15] rely on the experimental ones.

In Ref. [16] the SSD hypothesis was studied considering an exact treatment of the energy denominators of the perturbation theory. It was found that the $2\nu\beta\beta$ half-lives are reduced by a factor of about 20% for ground-state to ground-state transitions. It was also shown that by measuring the single-electron spectra and/or the angular distributions of the emitted electrons, the SSD hypothesis could be confirmed or ruled out experimentally in the near future.

In the last years, experimental information on the low-lying Gamow-Teller strength coming from charge-exchange reactions has been collected for several nuclei relevant to double-beta decay processes [17, 18, 19, 20, 21]. In particular, (p,n) reactions were used in Ref. [18] to study the transitions ^{128}Te$(0^+) \rightarrow {}^{128}I(1^+)$, the (^{3}He,$t$) reaction was used in Ref. [19] to study the transitions ^{100}Mo$(0^+) \rightarrow {}^{100}Tc(1^+)$ and ^{116}Cd$(0^+) \rightarrow {}^{116}In(1^+)$. The (p,n) reaction was also used in Ref. [20] to study ^{116}Cd$(0^+) \rightarrow {}^{116}In(1^+)$. Similarly, the reaction (d,^{2}He) was used in Ref. [21] to study the transitions ^{116}Sn$(0^+) \rightarrow {}^{116}In(1^+)$. These measurements complement the experimental information already available on the ft values for the transitions from the 1^+ ground state of the odd-odd intermediate nucleus to the 0^+ ground states of parent and daughter nuclei. In addition, they give information on the transitions to the 1^+ excited states of the intermediate nucleus.

In this paper we use a formalism based on a pnQRPA approach with a selfconsistent quasiparticle basis obtained from deformed Skyrme Hartre-Fock calculations with pairing correlations [22]. On top of that we include separable residual spin-isospin interactions in both particle-hole and particle-particle channels [23]. Within this formalism we calculate the GT strength distributions of the single beta branches as well as the $2\nu\beta\beta$ matrix elements corresponding to the double-beta emitters ^{100}Mo, ^{116}Cd, and ^{128}Te. With these results, we first evaluate to what extent the SSD hypothesis or the more relaxed low-lying states dominance (LLSD) hypothesis are fulfilled within our theoretical approach. Comparison with the available experimental information on both single-beta branches, EC/β^-, and $2\nu\beta\beta$ decay is also made. Finally, we extend the LLSD analysis to the rest of the observed $2\nu\beta\beta$ emitters, where the ground state of the intermediate nucleus is not 1^+, and we evaluate the contributions to the $2\nu\beta\beta$ half-lives considering an increasing range of excitation energy in the intermediate nucleus. Former calculations of running sums of matrix elements as a function of the excitation energy of the 1^+ intermediate nucleus were presented in Refs. [24, 25]. In Ref. [24] the results presented were for ^{76}Ge and were obtained within a phenomenological Woods-Saxon mean-field approach. In Ref. [25] results were presented for ^{36}Ar, ^{54}Fe, and ^{58}Ni within a shell model approach.

The paper is organized as follows. In Sec. II we present briefly the main formalism and discuss various approximations. In Sec. III we compare our results with experiment in the cases of ^{100}Mo, ^{116}Cd, and ^{128}Te and analyze the possible realizations of SSD and LLSD hypotheses. We also study in this section the single electron energy distributions of the outgoing electrons in the $2\nu\beta\beta$ decay processes with an exact treatment of the energy denominators. In Sec. IV we study the contributions of the different energy ranges to the $2\nu\beta\beta$ matrix elements in all the observed $2\nu\beta\beta$ emitters and discuss them in terms of LLSD. Finally we present in Sec. V the summary and the main conclusions.

II. BRIEF DESCRIPTION OF THEORETICAL CALCULATIONS

The double-beta decay is a nuclear process characterized by a change of two units in the nuclear charge, while the atomic mass number remains unchanged. Here we focus on the $2\nu\beta^-\beta^-$ decay mode where two antineutrinos and two electrons are emitted,

$$(Z,A)_{0_i^+} \rightarrow (Z+2,A)_{0_f^+} + 2e^- + 2\bar{\nu}_e \,. \tag{1}$$

Only the basic expressions are written here, more details can be found in Refs. [24, 26]. The half-life of the $2\nu\beta\beta$ decay can be written as

$$\left[T_{1/2}^{2\nu\beta\beta}\left(0_{\rm gs}^+ \rightarrow 0_{\rm gs}^+\right)\right]^{-1} = G^{2\nu\beta\beta}\left|M_{GT}^{2\nu\beta\beta}\right|^2 \,, \tag{2}$$

where $G^{2\nu\beta\beta}$ is the phase-space integral [2, 5]. The nuclear matrix element $M_{GT}^{2\nu\beta\beta}$ contains all the information on the nuclear structure involved in the process. The theoretical formalism used here is the pnQRPA based on a selfconsistent mean field that allows for pairing and deformation. We refer to this formalism in short as deformed HF+BCS+QRPA. In this formalism the nuclear matrix element can be written as,

$$M_{GT}^{2\nu\beta\beta} = \sum_M \sum_{\mu_i,\mu_f} (-1)^M \frac{\langle 0_f^+ 0|\sigma_{-M}t^-|1_{\mu_f}^+ M\rangle \, \langle 1_{\mu_f}^+ M|1_{\mu_i}^+ M\rangle \, \langle 1_{\mu_i}^+ M|\sigma_M t^-|0_i^+ 0\rangle}{(\omega^{\mu_f}+\omega^{\mu_i})/2} \,, \tag{3}$$

where the intermediate states are the 1^+ excitations of the initial and final nuclei in the laboratory frame. We use the Bohr-Mottelson factorization [27] for the total angular momentum states I^+ in the laboratory frame. The index $\mu_i(\mu_f)$ in Eq. (3) contains the $K_i(K_f)$ third component of the angular momentum of the QRPA state in the intrinsic system,

$$|I_{\mu_i}^+ M\rangle \equiv |I_{m_i}^+ K_i M\rangle = \sqrt{\frac{2I+1}{16\pi^2(1+\delta_{K_i,0})}}\left[D_{K_i M}^{\dagger\, I}(\Omega)|\phi_{K_i}^{m_i}\rangle + (-1)^{I-K_i} D_{-K_i M}^{\dagger\, I}(\Omega)|\bar{\phi}_{K_i}^{m_i}\rangle\right] \,, \tag{4}$$

with the intrinsic state

$$|\phi_{K_i}^{m_i}\rangle = \Gamma_{K_i}^{m_i}|\phi_{0,i}\rangle \qquad K_i = 0, \pm 1, \tag{5}$$

with $|\phi_{0,i}\rangle$ the QRPA vacuum of the initial state and $\Gamma_{K_i}^{m_i}$ the phonon QRPA operators. $|\bar{\phi}_{K_i}^{m_i}\rangle$ are the time reversed of $|\phi_{K_i}^{m_i}\rangle$. Similarly, the 0^+ initial and final states are of the Bohr-Mottelson form

$$|0_i^+ 0\rangle = \frac{1}{\sqrt{8\pi^2}} D_{00}^{\dagger\, 0}(\Omega)|\phi_{0,i}\rangle \,, \tag{6}$$

and similarly for the final state f. Integrating over the angular Ω variables, we finally obtain

$$M_{GT}^{2\nu\beta\beta} = \sum_{K=0,\pm 1} \sum_{m_i,m_f} (-1)^K \frac{\langle \phi_{0,f}|\sigma_{-K}t^-|\phi_K^{m_f}\rangle \, \langle \phi_K^{m_f}|\phi_K^{m_i}\rangle \, \langle \phi_K^{m_i}|\sigma_K t^-|\phi_{0,i}\rangle}{(\omega_K^{m_f}+\omega_K^{m_i})/2} \,. \tag{7}$$

As it is well known (see Ref. [28] and references therein) the Bohr-Mottelson factorization of the wave function gives the adiabatic limit of the exact angular momentum projection and is a very good approximation for well deformed nuclei. First order corrections to the Bohr-Mottelson factorization due to angular momentum projection are typically less than $1/\langle J_\perp^2\rangle$, where $\langle J_\perp^2\rangle$ is larger than 100 for well deformed nuclei [29]. In Eq. (7) $\omega_K^{m_i}(\omega_K^{m_f})$ are the RPA excitation energies of the intermediate 1^+ virtual states with respect to the initial (final) nucleus, with energy $E_i(E_f)$. The energy denominator is the average excitation energy of a couple of these intermediate states. The indices m_i, m_f run over all the 1^+ states of the intermediate nucleus $(Z+1,A)$ in the transition, and $K = 0, \pm 1$ are the

possible angular momentum projections of these intermediate states. The overlaps are needed to take into account the nonorthogonality of the intermediate states reached from initial and final ground states. Their expressions can be found in Refs. [24, 26].

To compute the matrix element we proceed as follows. Each initial and final even-even ground state is described as a pnQRPA vacuum. For each (N, Z) nucleus, a BCS ground state is independently obtained from a selfconsistent mean-field calculation on a large axially-symmetric harmonic oscillator basis, using a density-dependent effective interaction and a phenomenological pairing-gap parameter. The nucleon-nucleon effective force SLy4 [30] is used to generate the HF mean field, and the BCS equations are solved at each iteration with a value of the pairing gap obtained from even-odd experimental mass differences between neighboring nuclei [31]. When the iterative process converges, a set of single-particle states is obtained with their corresponding wave functions, energies, and occupation probabilities. It is worth noticing that the quadrupole deformation of the nucleus in its ground state is obtained selfconsistently as the shape that minimizes the nuclear energy. Separable Gamow-Teller particle-hole (ph) and particle-particle (pp) residual interactions are included and treated in pnQRPA [23]. The corresponding coupling constants χ_{ph} and κ_{pp} have been used in this work with values $\chi_{ph} = 20/A$ MeV and $\kappa_{pp} = 3/A$ MeV, which give a good description of GT properties when SLy4 Skyrme force is used, as we shall show in next section.

Due to the many-body approximations performed in the calculation, the intermediate 1^+ states computed from the initial and from the final ground states are different, and a projection from one basis to the other is in order. To get the $2\nu\beta\beta$ decay matrix element, every possible transition through all the intermediate 1^+ states is taken into account. The amplitude of each transition is divided by an energy denominator, as shown in Eq. (7). The energy denominators written in this way are obtained by replacing the lepton energies $E_{ei} + E_{\nu j}$, where E_e (E_ν) is the energy of the emitted electron (antineutrino), by an average quantity [2, 3, 4]

$$E_{ei} + E_{\nu j} \approx \frac{1}{2} Q_{\beta\beta} + m_e = \frac{1}{2}(E_i - E_f)\,, \tag{8}$$

where $Q_{\beta\beta}$ is the Q-value of the double-beta decay ($Q_{\beta\beta} = E_i - E_f - 2m_e$). E_i and E_f are the ground-state energies of parent and daughter nuclei, respectively. The consequences of this approximation on the SSD tests have been studied in Ref. [16]. We shall come back to this point in the next section. Different ways of writing these energy denominators, which are all equivalent, can be found in the literature. In particular one finds

$$\frac{1}{2}(\omega_K^{m_f} + \omega_K^{m_i}) = \frac{1}{2} Q_{\beta\beta} + E_m - E_i + m_e = E_m - \frac{1}{2}\left(E_i + E_f\right)\,, \tag{9}$$

where E_m is the energy of the intermediate nucleus in the state m. In the cases where the ground state of the intermediate nucleus is a 1^+ state, the denominator corresponding to the decay passing through this state can also be written as $(Q_{\beta^-} + Q_{\rm EC})/2$, where Q_{β^-} and $Q_{\rm EC}$ are the $Q-$values corresponding to its β^- and EC decay, respectively.

In this paper we study the contributions to the $2\nu\beta\beta$ nuclear matrix elements from consecutive terms in Eq. (7) with increasing energy denominators. The main purpose is to check the validity of the SSD hypothesis by considering only the lowest-energy term in the summation in the cases of ^{100}Mo, ^{116}Cd, and ^{128}Te, which are emitters with 1^+ intermediate ground states. However, it is also interesting to check the extent to which the contributions coming from low-lying virtual excitations are able to reproduce the total $2\nu\beta\beta$ nuclear matrix elements in a more general way. Actually, the strong fragmentation of the GT strength within the deformed formalism suggests that a meaningful comparison of theoretical results with experiment should be done for the accumulated strength in a given energy range rather than a direct comparison of individual excitations. Thus, we analyze the summation in Eq. (7) considering only the contribution of the intermediate ground state (to test SSD), then the contribution corresponding to all the low-lying states (to test LLSD), and finally taking into account all possible contributions (to get the complete result).

As mentioned before, in the cases where the ground state of the intermediate nucleus is a 1^+ state, we have experimental information on the β^- and EC decays of the ground state intermediate nucleus into the 0^+ ground states of the daughter and parent nuclei, respectively. We also have complementary experimental information based on charge-exchange reactions that can be evaluated and compared to the $2\nu\beta\beta$ experimental nuclear matrix element, as well as to the theoretical calculations. The contribution involving low-lying states can also be evaluated from the experimental information including now charge-exchange reactions [19, 21], and can be compared again with the total $2\nu\beta\beta$ experimental nuclear matrix element, as well as to the theoretical calculations.

III. RESULTS FOR $2\nu\beta\beta$ DECAYS WITH 1^+ GROUND STATE INTERMEDIATE NUCLEI

A. Single-state dominance

We start this section by summarizing the experimental situation concerning the validity of the SSD hypothesis in the $2\nu\beta\beta$ decay of ^{100}Mo, ^{116}Cd, and ^{128}Te. The analysis is based on information extracted from ground-state to ground-state decay measurements of the intermediate nuclei ^{100}Tc, ^{116}In, and ^{128}I, as well as on information extracted from charge-exchange reactions. Table I, II, and III contain the GT matrix elements for ground state to ground state transitions in the cases $A = 100$, $A = 116$, and $A = 128$, respectively. The notation used corresponds to the reaction point of view, where the $B(GT^-)$ strength corresponds to the $(Z, A) \rightarrow (Z+1, A)$ transition and the $B(GT^+)$ strength corresponds to the $(Z + 2, A) \rightarrow (Z + 1, A)$ transition. Thus, in the case of the decay of the intermediate nucleus, we still call $B(GT^-)$ to the strength corresponding to the EC/β^+ decay, and $B(GT^+)$ to the strength corresponding to the β^- decay, according to the following scheme:

$B(GT^-)$		$B(GT^+)$	
	$\underset{\longrightarrow}{\overset{EC}{\longleftarrow}}$ $(^3\mathrm{He}, t)$ (p, n)		$\underset{\longleftarrow}{\overset{\beta^-}{\longrightarrow}}$ $(d, ^2\mathrm{He})$ (n, p)	
^{100}Mo		^{100}Tc		^{100}Ru
^{116}Cd		^{116}In		^{116}Sn
^{128}Te		^{128}I		^{128}Xe

In this paper, results for $B(GT)$ are given in units in which the neutron decay has $B(GT)$=3. The matrix elements are extracted from the cross sections in the case of charge-exchange reactions [21] and from the $\log ft$ values in the case of the β decay :

$$M(GT) = \left[\frac{3D}{g_A^2\, ft}\right]^{1/2} , \tag{10}$$

where $D = 6147$ and $g_A = 1.25$ is the axial-vector coupling strength. The GT matrix element for the $2\nu\beta\beta$ decay within the SSD hypothesis is obtained from

$$M_{GT}^{2\nu\beta\beta}(SSD) = \frac{M(GT^-)M(GT^+)}{(Q_{\beta^-} + Q_{\mathrm{EC}})/2} = \frac{1}{\sqrt{ft_{\mathrm{EC}}}}\frac{1}{\sqrt{ft_{\beta^-}}}\frac{6D}{g_A^2(Q_{\beta^-} + Q_{\mathrm{EC}})} , \tag{11}$$

where the overlap in Eq. (7) has been approximated by one.

Table I shows the experimental Gamow-Teller matrix elements $M(GT^-)$ and $M(GT^+)$ for the transitions connecting the 1^+ ground state in ^{100}Tc with the 0^+ ground states in ^{100}Mo and ^{100}Ru. The $M(GT^-)$ matrix elements were extracted from (^{3}He,t) charge-exchange reactions [19] and from the ft_{EC} value as given in Ref. [12]. The $M(GT^+)$ matrix element was obtained from the ft_{β^-} value [32] in the decay ^{100}Tc $\rightarrow$ ^{100}Ru. The matrix elements $M_{GT}^{2\nu\beta\beta}$ are obtained from the two possible combinations of data. The half-lives $T_{1/2}^{2\nu\beta\beta}$ are calculated using approximated (SSD1) and exact (SSD2) energy denominators (we keep the notation used in previous references [16]). The experimental half-life is $T_{1/2}^{2\nu\beta\beta} = 7.1 \times 10^{18}$ y [33], which gives rise to a matrix element $(M_{GT}^{2\nu\beta\beta})_{\mathrm{exp}} = 0.241$ MeV^{-1}, using $g_A = 1.25$. One should notice that the half-lives are independent on the g_A value. As one can see in Table I, the agreement with the experimental half-life improves with SSD2 approach and it is particularly good when the matrix elements extracted from $\log ft$ are used.

Table II is similar to Table I but for A=116. Experimental values for $M(GT^-)$ are taken from (^{3}He,t) [19] and (p, n) [20] charge-exchange reactions, and from the ft_{EC} value for the decay of ^{116}In into the ground state of ^{116}Cd reported in Ref. [13]. Experimental values for $M(GT^+)$ are from Ref. [21], where the GT strength was extracted from the (d,^{2}He) charge-exchange reaction ^{116}Sn $\rightarrow$ ^{116}In. In this reference, the strength was normalized to recover at zero excitation energy the β^- decay data [34]. The results for $M_{GT}^{2\nu\beta\beta}$ are again compared to the values extracted from the

measured $2\nu\beta\beta$ decay half-life [33] ($T^{2\nu\beta\beta}_{1/2} = 3.0 \times 10^{19}$ y, and a corresponding matrix element $(M^{2\nu\beta\beta}_{GT})_{\rm exp} = 0.127$ MeV^{-1}, using $g_A = 1.25$). Except for the first row that contains the values extracted from (^{3}He,t) and that clearly overestimates the experimental half-life by almost one order of magnitude, we observe that both SSD1 and SSD2 half-lives underestimate the measured value.

Table III contains similar information for the case $A = 128$. Experimental values for $M(GT^-)$ are taken from the $ft_{\rm EC}$ value for the decay of ^{128}I into the ground state of ^{128}Te reported in Ref. [14], as well as from (p, n) reactions [18]. Experimental values for $M(GT^+)$ are taken from the ft_{β^-} value for the decay of ^{128}I into the ground state of ^{128}Xe [14]. In this case both SSD1 and SSD2 predictions overestimate the experimental half-life [33] ($T^{2\nu\beta\beta}_{1/2} = 2.5 \times 10^{24}$ y, and a corresponding matrix element $(M^{2\nu\beta\beta}_{GT})_{\rm exp} = 0.043$ MeV^{-1}, using $g_A = 1.25$).

B. Low-lying states dominance

In Tables IV, V, and VI, for the cases $A = 100$, $A = 116$, and $A = 128$ respectively, we show theoretical results and experimental data corresponding to the $B(GT^{\pm})$ strengths to the low-lying virtual states of the corresponding intermediate nuclei, as well as the contributions to $2\nu\beta\beta$ decay matrix element of the virtual transitions through them. A quenching factor $g_{A,\rm eff} = 0.8\, g_{A,\rm free}$ has been introduced in all the theoretical calculations reported in this paper, except for those shown later on in Fig. 6. In Table IV we do not have information on the low-lying $B(GT^+)$ strengths from charge-exchange reactions, only the $\log ft$ value is available. Thus, we only compute theoretical values for the $2\nu\beta\beta$ decay matrix element. We can see that the theoretical $B(GT^-)$ strengths accumulated up to 1.4 and 2.6 MeV, agree with the measurements [19] within a 80-90%. On the other hand, the $2\nu\beta\beta$ decay matrix element calculated up to 2.6 MeV of excitation energy in the intermediate nucleus accounts only for 65% of the experimental value.

In the case of $A = 116$ we can combine the experimental information available from (^{3}He,t) [19] and from (d,^{2}He) [21] to evaluate the $2\nu\beta\beta$ decay matrix element $M^{2\nu\beta\beta}_{GT}$ up to 3 MeV, and we can compare the obtained values with the total matrix element evaluated from the measured $2\nu\beta\beta$ half-life. Thus, we can test to what extent LLSD is valid in this case both theoretically and experimentally. First, we observe in Table V that the two single branches are reasonably reproduced by the calculations. In the case of $B(GT^+)$ the agreement is apparent. In the case of $B(GT^-)$ the comparison to experiment is not so meaningful because there is no agreement between experimental data from different groups [19, 20]. In particular, a very different value has been reported for the transition to the ground state. If we consider the new revised values given in Ref. [20] (see Table II), the agreement with the calculations clearly improves. The $2\nu\beta\beta$ decay matrix elements evaluated at increasing energies show first that they approach to the experimental value obtained from the $2\nu\beta\beta$ half-life (0.127 MeV^{-1}). We also observe that the theoretical results increase with energy to yield about a half of the experimental value at 3 MeV. Agreement improves when using the value of Ref. [20]. Table VI contains the results for $A = 128$. As in the case of $A = 100$, we do not have information on the low-lying $B(GT^+)$ strengths. Thus, we only compute theoretical values for the $2\nu\beta\beta$ decay matrix element.

Fig. 1 shows the accumulated single $B(GT^-)$ strength from ^{100}Mo $\rightarrow$ ^{100}Tc (upper panel), the accumulated single $B(GT^+)$ strength from ^{100}Ru $\rightarrow$ ^{100}Tc (middle panel) and the $2\nu\beta\beta$ GT matrix element from ^{100}Mo $\rightarrow$ ^{100}Ru (lower panel) in the low excitation energy range (up to 5 MeV). Available experimental data are shown by thick lines.

As one can see in Fig. 1 the theoretical $B(GT^-)$ strength below 3 MeV is rather fragmented, but the total accumulated strength agrees well with experiment. Although not shown in the figure, it is worth noticing that the GT resonance measured in Ref. [19] at 13-14 MeV with a strength $B(GT^-) = 23$ is well reproduced in our calculation, yielding a peak centered at 16 MeV with a similar strength. The strength obtained from the $\log ft$ value also agrees with the strength calculated up to about 0.5 MeV. In the case of the $B(GT^+)$ strength the only information comes from the $\log ft$ value at zero excitation energy. The corresponding strength is again well reproduced by the calculation of the accumulated strength below 0.5 MeV.

In the lower panel we show the theoretical calculation for the $2\nu\beta\beta$ matrix element as a function of the excitation energy taken into account in the sum in Eq. (7). It is compared with the experimental matrix element extracted from the measured $2\nu\beta\beta$ half-life. We compare our results with the values extracted from the measured $\log ft$ and charge-exchange reactions to check the validity of the SSD hypothesis graphically. We also show the total theoretical value when all the intermediate 1^+ states are considered in the calculation (see also Fig. 6). As can be seen in the lower panel, a rapid increase in the $2\nu\beta\beta$ decay matrix element takes place up to 2 MeV of intermediate excitation energy. It accounts for about 60% of the total matrix element. Eventually (see Fig. 6) the calculations reach the experiment when one considers the whole energy range. From the single-beta strengths one can see that there are no especially strong transitions to any low-energy intermediate state (in particular, to the ground state), which prevents the $2\nu\beta\beta$ matrix element from showing the same effect.

Summarizing, in the $2\nu\beta\beta$ decay of ^{100}Mo, the SSD hypothesis is fulfilled experimentally within 90%. The total theoretical $2\nu\beta\beta$ matrix element agrees well with experiment, while LLSD calculations up to 2 MeV account for 60%

of the experimental $2\nu\beta\beta$ matrix element. The remaining 40% comes from contributions of states at higher excitation energy.

Same results are shown for the transitions ^{116}Cd $\rightarrow$ ^{116}In (upper panel), ^{116}Sn $\rightarrow$ ^{116}In (middle panel) and ^{116}Cd $\rightarrow$ ^{116}Sn (lower panel) in Fig. 2. In the upper panel we show experimental data for $B(GT^-)$ from (^{3}He,t), together with the data at zero excitation energy extracted from (p,n), and from the log ft values. We also show the theoretical calculations that produce an increasing strength up to 1 MeV, which is very fragmented, but that finally reaches the most reliable experimental strength obtained from the measured log ft. In this case the GT resonance measured in Ref. [19] amounts to $B(GT^-) = 26$ and it is located at 14.5 MeV. Our calculation yields about the same strength centered at 16 MeV. The experimental data for $B(GT^+)$ are from (d,^{2}He) charge-exchange reactions [21], where the value extracted from β^- decay was used to normalize the strength.

The $B(GT^+)$ strength in the middle panel shows that the calculation reproduces the total experimentally measured strength below 3 MeV. The distribution of this strength is more fragmented in the calculations but the general trend is similar. In the lower panel we compare again our theoretical results for the $2\nu\beta\beta$ decay matrix element with experiment. In this case we compare with the experimental matrix element extracted from the measured half-life, as well as with the values extracted from the measured log ft values, and with the values extracted from charge-exchange reactions. We also show the total theoretical value (see also Fig. 6), which is very close to the experiment.

Theoretically, as in the case of $A = 100$, a strict SSD or LLSD is not observed in the lower panel. The few contributions below 1 MeV of excitation energy account for a 50% of the final value of the double-beta decay matrix element. Experimental accumulated single strengths are roughly in agreement with the results shown, but the double-beta experimental data for the low-energy contributions are, as in the case of $A = 100$, larger than our theoretical results.

Summarizing, in the $2\nu\beta\beta$ decay of ^{116}Cd there is no clear evidence that the SSD hypothesis is fulfilled experimentally because of the spread of data coming from different sources. The experimental LLSD up to 2.5 MeV accounts for the experimental $2\nu\beta\beta$ decay matrix element, while the calculations up to this energy account only for half of it. Since the total calculated matrix elements agrees well with experiment, the remaining contribution comes again from excited states at higher energies.

Fig. 3 is the corresponding figure for $A = 128$. In the upper panel we show experimental data for $B(GT^-)$ from (p,n), together with the data at zero excitation energy extracted from the log ft values. We also show the theoretical pnQRPA calculations. In this case the GT resonance measured in Ref. [18] contains a strength $B(GT^-) = 34.24$ located at 13.14 MeV. Our calculation yields $B(GT^-) = 35$ centered at 15 MeV. In the middle panel the experimental value at zero energy is obtained from log ft [14] and agrees well with the calculation (note the different scale as compared to the upper panel). The lower panel contains the results for the $2\nu\beta\beta$ decay matrix element. The meaning is the same as in the previous figures. We see that the total theoretical value (see also Fig. 6), is very close to the experiment and it is not reproduced by SSD or LLSD hypotheses.

A graphical representation of the calculations involved in Eq. (7) is shown in Fig. 4, featuring the theoretical 1^+ spectrum of the intermediate nucleus ^{100}Tc in the decay ^{100}Mo$\rightarrow$^{100}Ru in the left panel, the intermediate nucleus ^{116}In in the decay ^{116}Cd$\rightarrow$^{116}Sn in the middle panel, and the intermediate nucleus ^{128}I in the decay ^{128}Te$\rightarrow$^{128}Xe in the right panel. The vertical scale is the excitation energy of the intermediate nucleus, the horizontal scale represents the $B(GT)$ strength of the 1^+ QRPA states of the intermediate nucleus as obtained from the GT^- transitions in the initial double-beta emitter (shown from the central axis to the left), and from the GT^+ transitions in the final double-beta partner (shown from the central axis to the right). The larger this strength, the more relevant the corresponding contribution to the total double-beta decay matrix element, provided there are states coming from the other branch of the decay with similar wave functions (giving rise to non-negligible overlaps) and carrying non-negligible strengths.

C. Single electron energy distributions

In Ref. [16], the SSD hypothesis was tested using an exact treatment of the energy denominator in the nuclear matrix element, instead of the usual treatment of approximating the lepton energy by an average energy. It was shown that using the exact treatment of the energy denominator, the $2\nu\beta\beta$ decay half-life in the case of ^{100}Mo, is reduced by a factor of 20% for ground state to ground state decay. The single electron energy distributions of the outgoing electrons were also analyzed, and the predictions of different assumptions, SSD and higher state dominance (HSD)[16], were compared. In this work we extend this analysis to the case of pnQRPA theoretical calculations of the $2\nu\beta\beta$ decay rates with a correct treatment of the energy denominators and compare these predictions with those of SSD and HSD.

The formalism needed to calculate the differential $2\nu\beta\beta$ decay rates was developed in Ref. [16]. Here we only write the basic expressions used for the evaluation of the normalized decay rates.

The differential $2\nu\beta\beta$ decay rate to 0^+ ground state can be written as

$$dW = a_{2\nu} F(Z_f, E_{e1}) F(Z_f, E_{e2})\ \mathcal{M}\ d\Omega, \tag{12}$$

where $a_{2\nu} = (G_\beta g_A)^4 m_e^9/(64\pi^7)$ and $G_\beta = G_F \cos\theta_c$ (G_F is Fermi constant, θ_c is Cabbibo angle). $F(Z_f, E_e)$ denotes the relativistic Coulomb factor. The phase space factor is given by

$$\begin{aligned} d\Omega \ = \ & \frac{2}{m_e^{11}} E_{e1} p_{e1}\ E_{e2} p_{e2}\ E_{\nu 1}^2\ E_{\nu 2}^2\ \delta(E_{e1} + E_{e2} + E_{\nu 1} + E_{\nu 2} + E_f - E_i) \times \\ & dE_{e1}\ dE_{e2}\ dE_{\nu 1}\ dE_{\nu 2}. \end{aligned} \tag{13}$$

$\mathcal{M}$ consists of the products of nuclear matrix elements:

$$\mathcal{M} \ = \ \frac{m_e^2}{4} \left[|\mathcal{K} + \mathcal{L}|^2 + \frac{1}{3} |\mathcal{K} - \mathcal{L}|^2 \right], \tag{14}$$

where $\mathcal{K}(\mathcal{L})$ denotes nuclear matrix elements with an energy denominator given by K_m (L_m),

$$\begin{aligned} K_m &\equiv [E_m - E_i + E_{e1} + E_{\nu 1}]^{-1} + [E_m - E_i + E_{e2} + E_{\nu 2}]^{-1}, \\ L_m &\equiv [E_m - E_i + E_{e2} + E_{\nu 1}]^{-1} + [E_m - E_i + E_{e1} + E_{\nu 2}]^{-1}. \end{aligned} \tag{15}$$

The normalized total decay rate can be written as

$$P = \frac{1}{W} \frac{dW}{dE_e}, \tag{16}$$

where the full decay probability W is given by

$$\begin{aligned} W = & \frac{2 a_{2\nu}}{m_e^{11}} \int_{m_e}^{E_i - E_f - m_e} F(Z_f, E_{e1}) p_{e1} E_{e1} dE_{e1} \times \\ & \int_{m_e}^{E_i - E_f - E_{e1}} F(Z_f, p_{e2}) p_{e2} E_{e2} dE_{e2} \int_0^{E_i - E_f - E_{e1} - E_{e2}} \mathcal{M}\ E_{\nu 2}^2 E_{\nu 1}^2 dE_{\nu 1}\,. \end{aligned} \tag{17}$$

In Fig. 5 we present the single electron spectrum of the emitted electrons calculated within SSD, HSD, and total pnQRPA for the $2\nu\beta\beta$ of ^{100}Mo (upper panel) and ^{116}Cd (lower panel). The different behavior observed at small electron energies for different assumptions is of the order of few percent. This accuracy is now accessible in the NEMO-3 experiment [35], where a large amount of events for the $2\nu\beta\beta$ decay of ^{100}Mo has been collected.

IV. TEST OF LLSD IN DOUBLE-BETA EMITTERS

As an extension of the analysis of the SSD hypothesis, we have also studied the contributions to the $2\nu\beta\beta$ decay matrix element through the low-lying intermediate states for all confirmed $2\nu\beta\beta$ partners, also in the cases in which the ground state of the corresponding intermediate nucleus is not a 1^+ state. To this end, we plot in Fig. 6 for all the nuclei under study the $2\nu\beta\beta$ decay matrix elements as a function of the excitation energy of the intermediate nucleus taken into account in the calculation. As in the previous section, a deformed Skyrme-SLy4 HF mean field has been used to describe the initial and final ground states, with pairing correlations treated in BCS approximation. In general we use the ground states for initial and final nuclei with a shape that minimize the HF+BCS energy. The corresponding results are shown by the solid lines. In some instances like ^{48}Ti and ^{76}Se, the minima correspond to a spherical shape ($\beta = 0$), while experimental data [36] indicate that these nuclei have a non negligible deformation in the ground state ($\beta \sim 0.15$). In these cases we also show results obtained with the pnQRPA calculations based on the HF+BCS solutions corresponding to these non-zero deformations ($\beta = 0.17$ for ^{48}Ti and $\beta = 0.14$ for ^{76}Se). The corresponding results shown by dashed lines in Fig. 6 are seen to agree much better with experiment. It is important to remark that particularly in the case of ^{48}Ti, the HF+BCS energy has a rather shallow minimum in the deformation range from $\beta = 0$ to $\beta = 0.17$, so that both solutions are equally plausible ground states of ^{48}Ti. The grey area in the plots indicates the experimental range of the $2\nu\beta\beta$ decay matrix element. The two limiting horizontal lines have been deduced from experimental half-lives [33] using two different values of the constant g_A, namely g_A=1.25 (bare value) and g_A=1.00 (quenched value). In this case the theoretical results are not quenched.

Typically, the $2\nu\beta\beta$ decay matrix elements shown in the plots increase with the excitation energy of the intermediate states until they reach a constant value right after a rather prominent final step located between 15 and 20 MeV. This last step, especially important for the double-beta partners with $A = 128$, 130 and 136, is related to the GT^- giant resonance. The final value of the $2\nu\beta\beta$ decay matrix element lies within the experimental region in most cases. Important deviations are only found for the nuclei with $A = 130$ and 136. In the cases of $A = 48$ and $A = 76$, as already mentioned, the prolate shapes of the daughter nuclei give a better result than the spherical shapes. Concerning the low energy contributions to the matrix element, the fastest increase appears in the double-beta partners with $A = 48$, 96, 100, and 116, where around a 60% of the total matrix element is reached within an excitation energy range of 2 MeV, and to a lesser extent the A=150 case. In the other double-beta partners the contributions to the matrix element are more spread and the increase is slower. In general, important contributions appear from relatively high energies around the position of the GT resonance. Thus, although neither SSD nor LLSD hypotheses are clearly fulfilled in our theoretical results, one can see a tendency in most cases to exhaust at least 50% of the total $2\nu\beta\beta$ matrix elements in a low excitation energy region of 5 MeV. The only salient exceptions to this rule are the cases of A=82, 130, and 136.

V. CONCLUSIONS

In this work we have studied the $2\nu\beta\beta$ decay matrix elements within a selfconsistent Skyrme Hartree-Fock calculation with pairing and deformation, and with residual *ph* and *pp* interactions treated in pnQRPA. The analysis has been focused on the study of the validity of SSD and LLSD. While the former has been tested on the $2\nu\beta\beta$ decay of ^{100}Mo, ^{116}Cd, and ^{128}Te, the latter has been checked on all the measured $2\nu\beta\beta$ emitters. Confirmation of that hypothesis has important consequences both experimentally and theoretically, since it could help to drastically simplify the experimental effort to get good estimates of $2\nu\beta\beta$ half-lives on one hand, and to simplify the theoretical description of the intermediate nucleus on the other.

With this aim, we have studied first the $B(GT^{\pm})$ strength distributions of the intermediate $2\nu\beta\beta$ nuclei ^{100}Tc, ^{116}In, and ^{128}I in the low range of excitation energies, comparing the theoretical results with the available experimental information from the direct decay and from charge-exchange reactions. The calculations reproduce fairly well the experimental distributions at low energy as well as the position and total strength of the GT resonances.

The result of the analysis performed concludes that SSD is experimentally realized in the case of ^{100}Mo because its experimental $2\nu\beta\beta$ half-life is roughly accounted for by the measured $B(GT)$ strengths connecting the ground states of the nuclei involved. On the contrary, the SSD half-lives are underestimated in the case of ^{116}Cd and are overestimated in the case of ^{128}Te. However, these results are still not conclusive since the uncertainties arising from the insufficient precision of the experimental measurements of ft-values, of $2\nu\beta\beta$ half-lives, and especially because of the uncertainties of the $B(GT)$ strength extracted from charge-exchange reactions.

From the theoretical side, the conclusion of our results is that clear evidences for SSD and LLSD are not found within the present approach. This is at variance with the conclusion in Ref. [15], where strong support of SSD was claimed. However, we would like to point out that our theoretical LLSD $2\nu\beta\beta$ matrix elements agree up to factors of the order of 2 with our total matrix elements. This finding is in qualitative agreement with the results obtained in previous studies [15, 16]. Furthermore, in Ref. [15] it is stated that SSD results agree quite well with the total matrix elements even though they find in some cases discrepancies up to a factor of 2.

With only two exceptions (A=130, 136), our calculations reproduce the experimental $2\nu\beta\beta$ half-lives when the whole energy range of excitation energies in the intermediate nucleus is considered. Within the considered nuclear model we find that important contributions to the $2\nu\beta\beta$ decay matrix elements arise from relatively high excitation energies in several cases, not supporting dominance of single or even low-lying states. Further progress in both experimental and theoretical sides is still needed to clarify the importance of the contributions of the intermediate nucleus states to the $2\nu\beta\beta$ decay matrix elements. In the experimental case, this progress can be achieved by completing the experiments with high resolution charge-exchange reactions to more nuclei of interest and extending the measurements of GT strength distributions up to the resonance regions. For further progress in the field, measurements of the occupation numbers in particle-transfer reactions [37] are also of great importance. In the theoretical case improvements are needed in the treatment of the residual forces by using realistic interactions and improved parametrizations, especially in the particle-particle sector. The role of the axial-vector coupling strength should be also studied further because systematic indications in favor of strong quenching have been recently reported [38].

The single electron energy distributions of the outgoing electrons in the $2\nu\beta\beta$ decay processes have been investigated under various assumptions (SSD, HSD), as well as from theoretical calculations using an exact treatment of the energy denominators of the perturbation theory, i.e., without factorization of the nuclear structure and phase space integration calculations. A more comprehensive analysis of NEMO-3 data including the theoretical predictions presented in this paper could help to confirm or rule out the possible realizations of SSD and LLSD.

Acknowledgments

This work was supported by Ministerio de Ciencia e Innovación (Spain) under Contract No. FIS2005-00640. It was also supported in part by the EU ILIAS project under contract RII3-CT-2004-506222. O.M. and R.A.R. thank Ministerio de Ciencia e Innovación (Spain) for financial support.

---

[1] Fukuda Y *et al* 1998 *Phys. Rev. Lett.* **81** 1562
Ahn M H *et al* 2006 *Phys. Rev.* D **74** 072003
Ahmad Q R *et al* 2002 *Phys. Rev. Lett.* **89** 011301
Ahmad Q R *et al* 2002 *Phys. Rev. Lett.* **89** 011302
Araki T *et al* 2005 *Phys. Rev. Lett.* **94** 081801
[2] Suhonen J and Civitarese O 1998 *Phys. Rep.* **300** 123
[3] Faessler A and Šimkovic F 1998 *J. Phys. G: Nucl. Part. Phys.* **24** 2139
[4] Elliott S and Vogel P 2002 *Ann. Rev. Nucl. Part. Phys.* **52** 115
[5] Haxton W C and Stephenson Jr. G J 1984 *Prog. Part. Nucl. Phys.* **12** 409
[6] Caurier E, Nowacki F, Poves A and Retamosa J 1996 *Phys. Rev. Lett.* **77** 1954
[7] Halbeib J A and Sorensen R A 1967 *Nucl. Phys.* A **98** 542
[8] Engel J, Vogel P and Zirnbauer M R 1988 *Phys. Rev.* C **37** 731
[9] Muto K and Klapdor H V 1988 *Phys. Lett.* B **201** 420
[10] Suhonen J, Taigel T and Faessler A 1988 *Nucl. Phys.* A **486** 91
[11] Abad J, Morales A, Nuñez-Lagos R, Pacheco A F 1984 *An. Fis.* A **80** 9
[12] García A *et al* 1993 *Phys. Rev.* C **47** 2910
[13] Bhattacharya M *et al* 1998 *Phys. Rev.* C **58** 1247
[14] Kanbe M and Kitao K 2001 *Nucl. Data Sheets* **94** 227
[15] Civitarese O and Suhonen J 1998 *Phys. Rev.* C **58** 1535
Civitarese O and Suhonen J 1999 *Nucl. Phys.* A **653** 321
[16] Domin P, Kovalenko S, Šimkovic F and Semenov S V 2005 *Nucl. Phys.* A **753** 337
Šimkovic F, Domin P and Semenov S V 2001 *J. Phys. G: Nucl. Part. Phys.* **27** 2233
[17] Rakers S *et al* 2004 *Phys. Rev.* C **70** 054302
Grewe E W *et al* 2006 *Prog. Part. Nucl. Phys.* **57** 260
Grewe E W *et al* 2007 *Phys. Rev.* C **76** 054307
Grewe E W *et al* 2008 *Phys. Rev.* C **77** 064303
[18] Madey R *et al* 1989 *Phys. Rev.* C **40** 540
[19] Akimune H, Ejiri H, Fujiwara M, Daito I, Inomata T, Hazama R, Tamii A, Toyokawa H and Yosoi M 1997 *Phys. Lett.* B **394** 23
[20] Sasano M*et al* 2007 *Nucl. Phys.* A **788** 76c
[21] Rakers S *et al* 2005 *Phys. Rev.* C **71** 054313
[22] Vautherin D and Brink D M 1972 *Phys. Rev.* C **5** 626
Vautherin D 1973 *Phys. Rev.* C **7** 296
[23] Sarriguren P, Moya de Guerra E, Escuderos A and Carrizo A C 1998 *Nucl. Phys.* A **635** 55
Sarriguren P, Moya de Guerra E and Escuderos A 1999 *Nucl. Phys.* A **A58** 13
Sarriguren P, Moya de Guerra E and Escuderos A 2001 *Nucl. Phys.* A **A691** 631
Sarriguren P, Moya de Guerra E and Escuderos A 2001 *Phys. Rev.* C **64** 064306
[24] Šimkovic F, Pacearescu L and Faessler A 2004 *Nucl. Phys.* A **733** 321
[25] Nakada H, Sebe T and Muto K 1996 *Nucl. Phys.* A **607** 235
[26] Álvarez-Rodríguez R, Sarriguren P, Moya de Guerra E, Pacearescu L, Faessler A and Šimkovic F 2004 *Phys. Rev.* C **70** 064309
[27] Bohr A and Mottelson B 1975 *Nuclear Structure* (Benjamin, New York)
[28] Moya de Guerra E 1986 *Phys. Rep.* **138** 293
Villars F 1966 *Many-body description of nuclear structure and reactions*, ed. C. Bloch (Academic Press, N.Y.)
[29] Moya de Guerra E and Kowalski S 1979 *Phys. Rev.* C **20** 357
Berdichevsky D, Sarriguren P, Moya de Guerra E, Nishimura M, and Sprung D W L 1988 *Phys. Rev.* C **38** 338
Sarriguren P, Graca E, Sprung D W L, Moya de Guerra E and Berdichevsky D 1989 *Phys. Rev.* C **40** 1414
[30] Chabanat E, Bonche P, Haensel P, Meyer J and Schaeffer R 1998 *Nucl. Phys.* A **635** 231
[31] Audi G, Bersillon O, Blachot J and Wapstra A H 2003 *Nucl. Phys.* A **729** 3
[32] Singh B 2008 *Nucl. Data Sheets* **109** 297
[33] Barabash A S 2002 *Czech. J. Phys.* **52** 567
Barabash A S 2006 arXiv:nuclex/0602009v2
[34] Blachot J 2001 *Nucl. Data Sheets* **92** 455

[35] Arnold R *et al* 2005 *Phys. Rev. Lett.* **95** 182302
Arnold R *et al* 2007 *Nucl. Phys.* A **781** 209
[36] Raghavan P 1989 *Atomic and Nuclear Data Tables* **42** 189
Stone N J 2001 *Table of Nuclear Moments* www.nndc.bnl.gov/nndc/stone_moments
[37] Freeman S J *et al* 2007 *Phys. Rev.* C **75** 051301(R)
Schiffer J P *et al* 2008 *Phys. Rev. Lett.* **100** 112501
[38] Faessler A, Fogli G L, Lisi E, Rodin V, Rotunno A M and Šimkovic F 2008 *J. Phys. G: Nucl. Part. Phys.* **35** 075104

TABLE I: Experimental Gamow-Teller matrix elements $M(GT^-)$ and $M(GT^+)$ for the transitions connecting the 1^+ ground state in ^{100}Tc with the 0^+ ground states in ^{100}Mo and ^{100}Ru. We also show the matrix elements $M_{GT}^{2\nu\beta\beta}$ [MeV^{-1}] and the corresponding half-lives $T_{1/2}^{2\nu\beta\beta}$ [y] obtained with aproximated (SSD1) and exact (SSD2) energy denominators. The experimental half-life is $T_{1/2}^{2\nu\beta\beta} = 7.1 \times 10^{18}$ y [33], and its corresponding matrix element is $(M_{GT}^{2\nu\beta\beta})_{\rm exp} = 0.241$ MeV^{-1}. While the half-lives are independent on g_A, the matrix elements have been obtained using g_A=1.25.

$M(GT^-)$	$M(GT^+)$	$M_{GT}^{2\nu\beta\beta}$	$T_{1/2}^{2\nu\beta\beta}$ (SSD1)	$T_{1/2}^{2\nu\beta\beta}$ (SSD2)
0.57[a]	0.55[b]	0.19	1.1 $\times 10^{19}$	8.8 $\times 10^{18}$
0.65[c]	0.55[b]	0.21	9.3 $\times 10^{18}$	7.2 $\times 10^{18}$

[a] from (^{3}He,t) [19]
[b] from $\log ft_{\beta-}$ [32]
[c] from $\log ft_{\rm EC}$ [12]

TABLE II: Same as Table I, but for $A = 116$. In this case the $2\nu\beta\beta$ half-life is $T_{1/2}^{2\nu\beta\beta} = 3 \times 10^{19}$ y [33], and its corresponding matrix element is $(M_{GT}^{2\nu\beta\beta})_{\rm exp} = 0.127$ MeV^{-1}.

$M(GT^-)$	$M(GT^+)$	$M_{GT}^{2\nu\beta\beta}$	$T_{1/2}^{2\nu\beta\beta}$ (SSD1)	$T_{1/2}^{2\nu\beta\beta}$ (SSD2)
0.18[a]	0.51[b]	0.05	1.9 $\times 10^{20}$	1.7 $\times 10^{20}$
0.51[c]	0.51[b]	0.14	2.4 $\times 10^{19}$	2.1 $\times 10^{19}$
0.69[d]	0.51[b]	0.19	1.3 $\times 10^{19}$	1.2 $\times 10^{19}$

[a] from (^{3}He,t) [19]
[b] from $\log ft_{\beta-}$ [34], used by [21]
[c] from (p,n) [20]
[d] from $\log ft_{\rm EC}$ [13]

TABLE III: Same as Table I, but for $A = 128$. In this case the $2\nu\beta\beta$ half-life is $T_{1/2}^{2\nu\beta\beta} = 2.5 \times 10^{24}$ y [33], and its corresponding matrix element is $(M_{GT}^{2\nu\beta\beta})_{\rm exp} = 0.043$ MeV^{-1}.

$M(GT^-)$	$M(GT^+)$	$M_{GT}^{2\nu\beta\beta}$	$T_{1/2}^{2\nu\beta\beta}$ (SSD1)	$T_{1/2}^{2\nu\beta\beta}$ (SSD2)
0.41[a]	0.10[b]	0.024	8.1 $\times 10^{24}$	7.8 $\times 10^{24}$
0.33[c]	0.10[b]	0.019	1.3 $\times 10^{25}$	1.2 $\times 10^{25}$

[a] from (p,n) [18]
[b] from $\log ft_{\beta-}$ [14]
[c] from $\log ft_{\rm EC}$ [14]

TABLE IV: Theoretical (quenched) and experimental accumulated single Gamow-Teller strengths $B(GT^-)$ and $B(GT^+)$ up to the different measured excitation energies of the intermediate nucleus. The corresponding values of the double GT matrix element $M_{GT}^{2\nu\beta\beta}$ [MeV^{-1}] up to the same excitation energies for ^{100}Mo $\rightarrow^{100}$Ru are also given.

	$\sum$ B(GT$^-$)		$\sum$ B(GT$^+$)		$M_{GT}^{2\nu\beta\beta}$	
E [MeV]	th.	exp.[a]	th.	exp.	th.	exp.
1.4	0.42	0.46	0.73	-	0.12	-
2.6	0.53	0.69	1.26	-	0.15	-

[a] from (^{3}He,t) [19]

TABLE V: Same as in Table IV, but for $A = 116$.

	$\sum$ B(GT$^-$)		$\sum$ B(GT$^+$)		$M_{GT}^{2\nu\beta\beta}$	
E [MeV]	th.	exp.[a]	th.	exp.[b]	th.	exp.
0.7	0.29	0.03	0.50	0.33	0.03	0.05
1.0	0.56	0.15	0.56	0.44	0.06	0.09
2.2	0.56	0.32	0.69	<0.51	0.06	<0.12
3.0	0.56	0.32	0.75	<0.72	0.06	<0.12

[a] from (^{3}He,t) [19]
[b] from (d,^{2}He) [21]

TABLE VI: Same as in Table IV, but for $A = 128$.

	$\sum$ B(GT$^-$)		$\sum$ B(GT$^+$)		$M_{GT}^{2\nu\beta\beta}$	
E [MeV]	th.	exp.[a]	th.	exp.	th.	exp.
0.58	0.004	0.22	0.014	-	0.000	-
1.09	0.094	0.52	0.021	-	0.004	-
1.61	0.382	0.64	0.027	-	0.012	-
2.56	0.468	1.07	0.187	-	0.021	-

[a] from (p, n) [18]

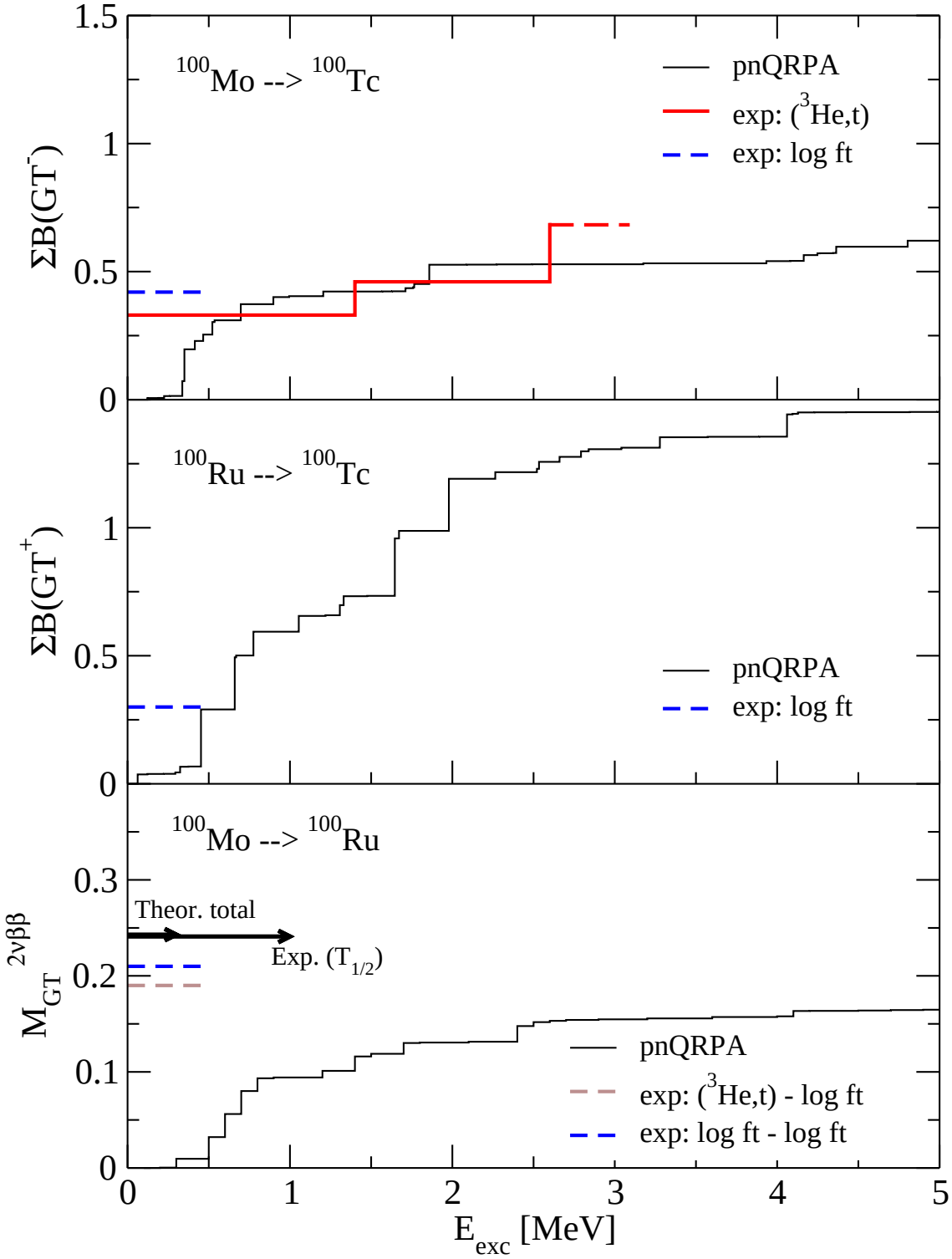

FIG. 1: Accumulated $B(GT^-)$ strength for the transition ^{100}Mo→^{100}Tc (upper panel), accumulated $B(GT^+)$ strength for the transition ^{100}Ru→^{100}Tc (middle panel) and $M_{GT}^{2\nu\beta\beta}$ [MeV^{-1}] matrix element for the transition ^{100}Mo→^{100}Ru (lower panel) as a function of the excitation energy of the intermediate nucleus from a HF+BCS+QRPA calculations, together with experimental data from various sources.

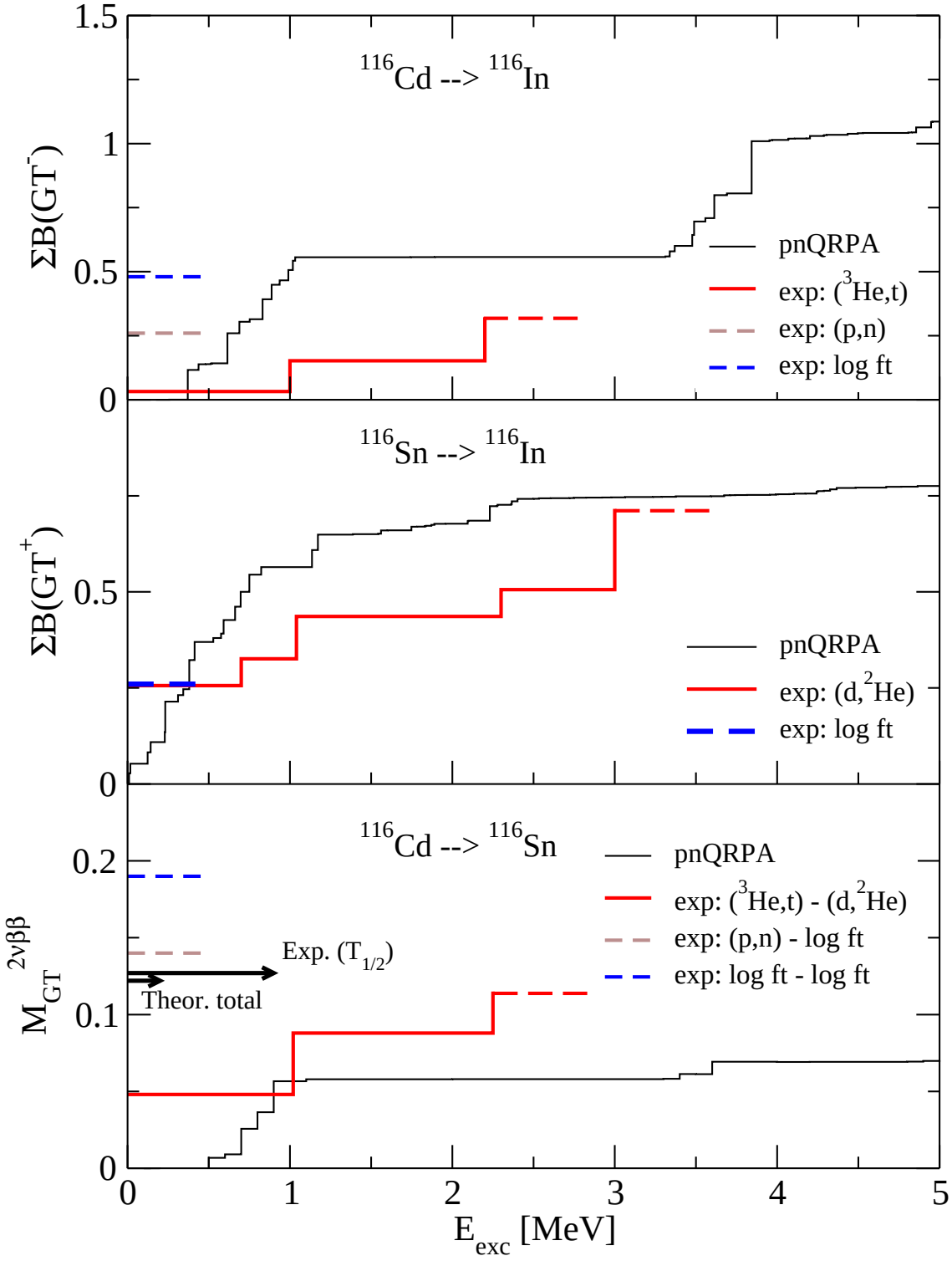

FIG. 2: Same as in Fig. 1, but for the transition ^{116}Cd→^{116}Sn.

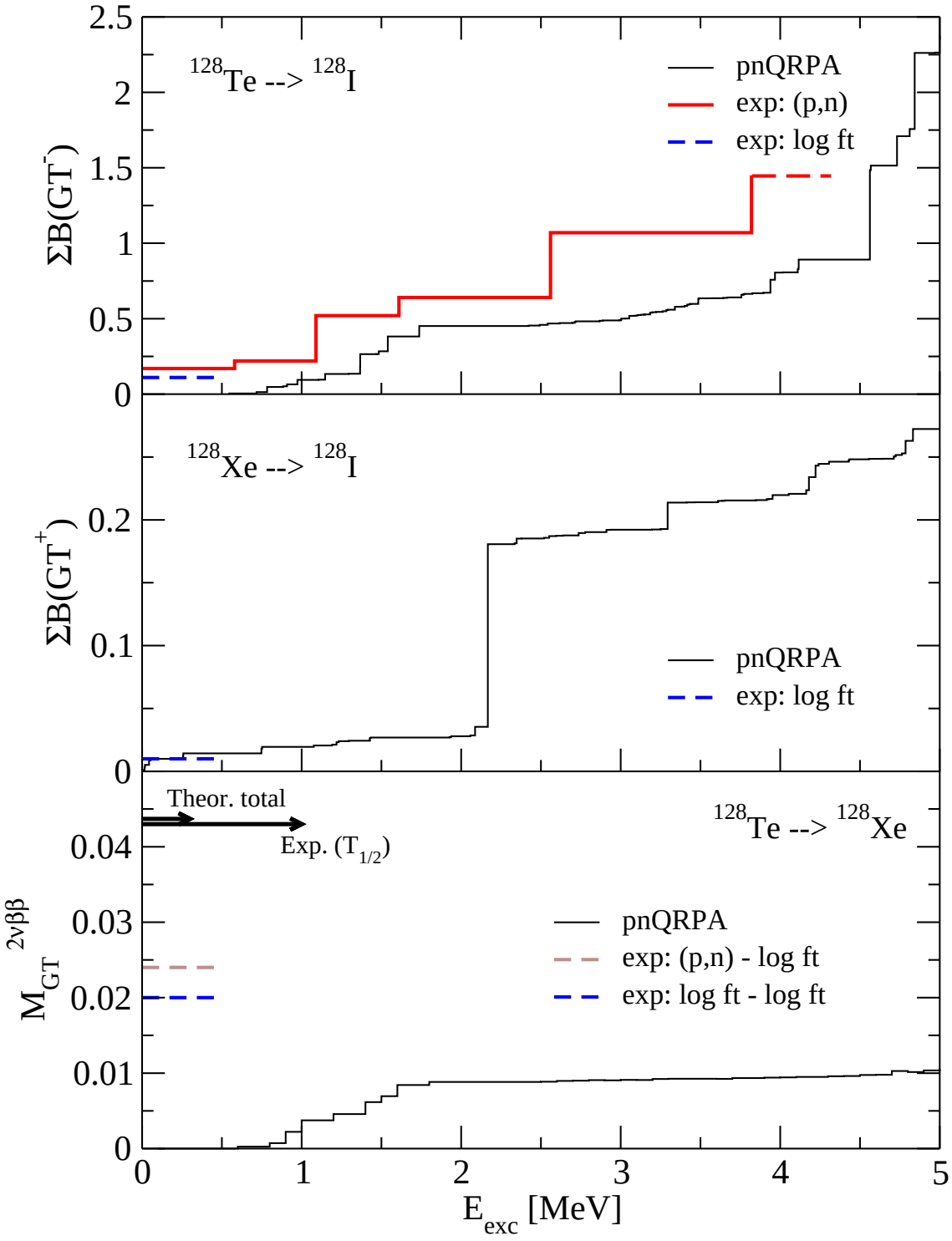

FIG. 3: Same as in Fig. 1, but for the transition ^{128}Te→^{128}Xe.

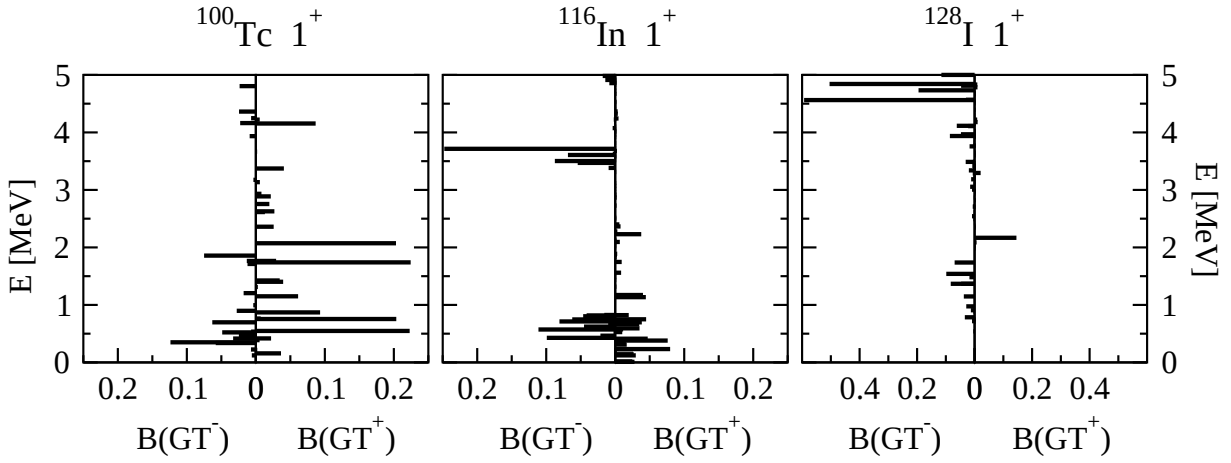

FIG. 4: $B(GT^{\pm})$ strength distributions in the intermediate nucleus ^{100}Tc (left), ^{116}In (middle), and ^{128}I (right) of the double-beta decay ^{100}Mo$\rightarrow^{100}$Ru, ^{116}Cd$\rightarrow^{116}$Sn, and ^{128}Te$\rightarrow^{128}$Xe, respectively.

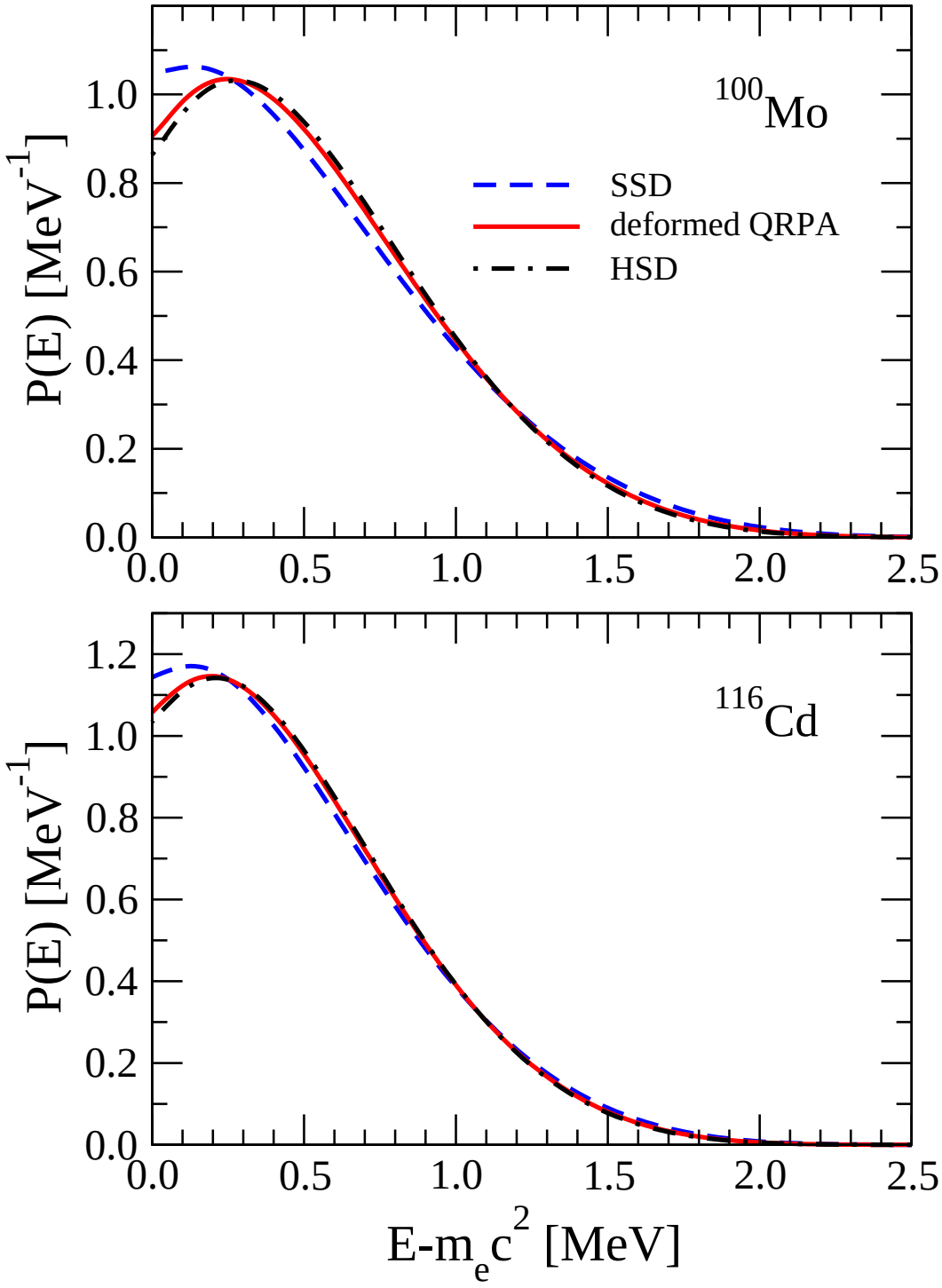

FIG. 5: Single electron differential decay rate normalized to the total decay rate for the $2\nu\beta\beta$ decay to the 0^+ ground state in ^{100}Mo$\rightarrow^{100}$Ru (upper panel) and ^{116}Cd$\rightarrow^{116}$Sn (lower panel).

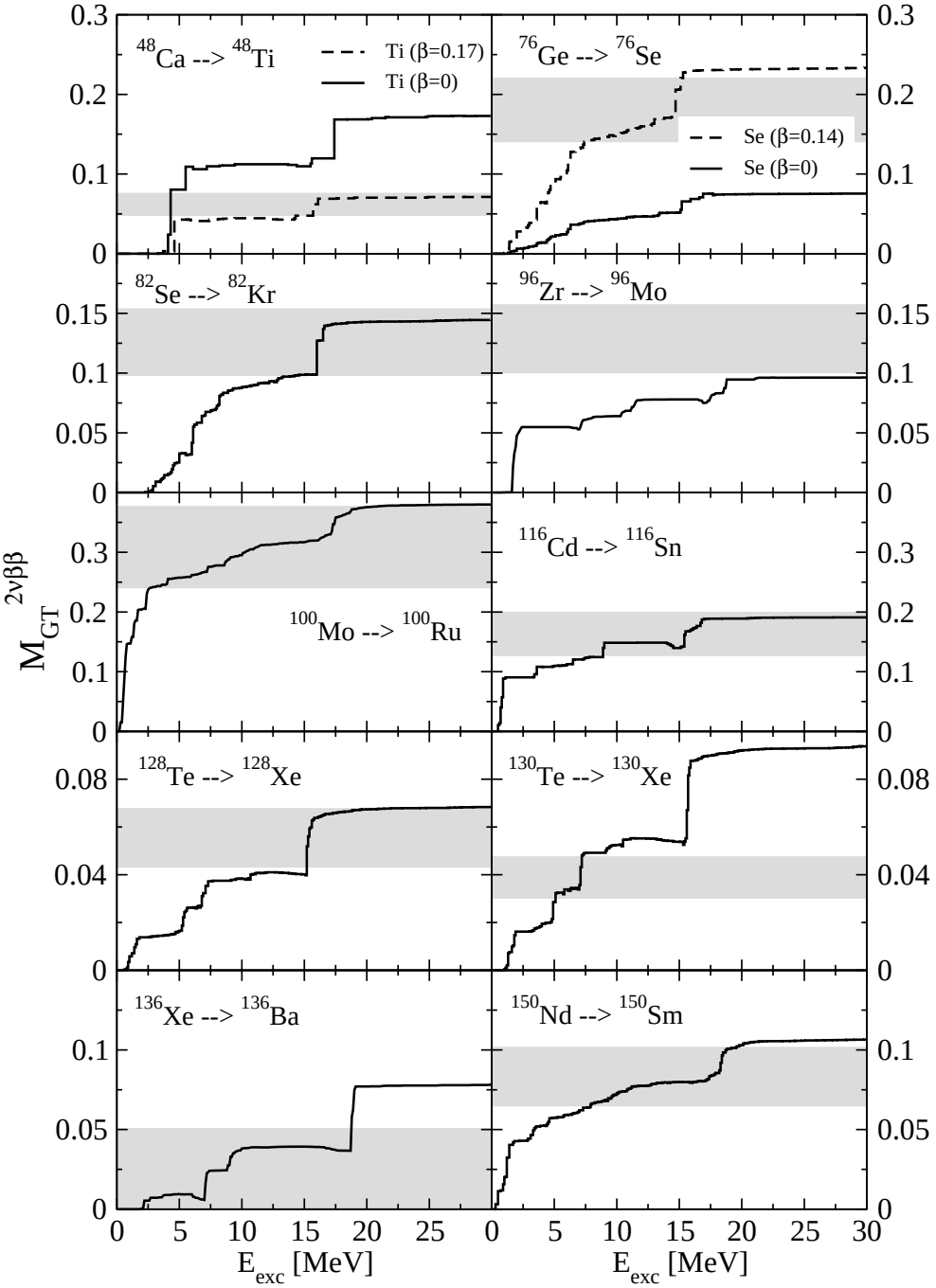

FIG. 6: Double-beta decay matrix elements as a function of the intermediate nucleus excitation energy considered in the calculation. An experimental range is given by a shadow area where the upper and lower limits are deduced from the experimental half-lives [33], using g_A =1.00 and g_A =1.25, respectively. Dashed lines in $A = 48$ and $A = 76$ correspond to calculations with an alternative choice of deformation (see text).